

# Wireless Sensing for Ground Engaging Tools

M. Adel Ibrahim<sup>1</sup>, Galal Hassan<sup>2</sup>, Hossam S. Hassanein<sup>3</sup>, Khaled Obaia<sup>4</sup>

<sup>1</sup>Electrical & computer engineering, Queen's University, Kingston, Canada

<sup>2,3</sup>School of computing, Queen's University, Kingston, Canada

<sup>4</sup>Oil & Gas, Edmonton, Canada

{<sup>1</sup>mibrahim, <sup>2</sup>ghassan, <sup>3</sup>hossam}@cs.queensu.ca, <sup>4</sup>obaia.khaled@syncrude.com

**Abstract**—In this work, we discuss the problem of accidentally detached Ground Engaging Tools (GETs). We overview potential solutions and demonstrate the design and implementation of a hardware sensing platform and a Wireless Sensor Network (WSN) for monitoring the GETs of an electric-rope shovel digging in an oil-sand mine. The designed system utilize a rugged hardware sensing platform equipped with a myriad of sensors monitoring mechanical integrity and shovel utilization. Field testing on an operational shovel allowed for collecting and analyzing real sensory data to evaluate the system's performance. All emulated detachments events were successfully detected and reported by the system.

**Index Terms**—wireless sensor networks, ground engaging tools (GETs), digging equipment, construction, mining, agriculture, hardware platform, shovel teeth.

## I. INTRODUCTION

With the imminent arrival of industry 4.0 [1], [2], distributed automation plays a crucial role in modern industrial processes. Industrial Internet of Things (IIoT) in general, and Wireless Sensor Networks (WSNs) in particular are key enablers of distributed automation. WSNs allow for collecting sensory data from places previously considered inaccessible. Albeit their known challenges [3], WSNs has the potential to extend the reach of digital control to unprecedented domains.

Construction, mining, and agricultural equipment can benefit significantly from WSNs. Large fleets of earth processing equipment regularly consume significant amounts of ground engaging tools (GETs) such as shovel teeth, side cutters, dozer blades, rippers, chisels, hammers, and the list goes on.

All these GETs have two main functions. First, to allow for sufficient pressure build-up at their tips to pierce and break the ground. Second, to act as sacrificial pieces and mechanical shields protecting a more expensive part in the equipment. Both of these functions expose GETs to significant abrasive wear [4] and fatigue [5] during operation. Consequently, they require regular replacement.

When a GET approaches the end of its service life (almost worn out), it becomes prone to structural failures which often result in its detachment from the equipment. Typically, the GET is a heavy chunk of steel which can cause a lot of damage if it ends up in the wrong place.

Conventionally, the responsibility of monitoring the GET is assigned to the operator. Needless to say that during active operations, a typical equipment operator will have enough visual and audible stimulation to saturate their senses and limit their capability to monitor their own GETs. Also, sometimes

the operator may not have visual access to the GETs from the cabin. This has contributed to numerous events of broken/detached GETs going unnoticed and causing significant equipment damage and in some cases human injury [6]. The maintenance cost and the production losses varies greatly from a few thousands to millions of dollars depending on the type and scale of damage caused by the broken GET.

In this work we discuss the two approaches proposed for monitoring GETs. We favour one approach over the other explaining the reasons. Then we introduce our case study and demonstrate the design and implementation of a complete system for monitoring the GETs of an electric-rope shovel. The presented system is a WSN utilizing a rugged sensing platform to measure the close proximity of the GET to the shovel's bucket during operation. When a detachment is detected, the system alarms the operator and specifies the location of the missing GET.

In section II, we discuss the camera approach vs the WSN approach. Section III introduces the case study. The hardware design of the Sensor Node (SeN) is presented in section IV. Then, section V discusses the hardware setup of the Sink Node (SiN). Finally, the field test results are presented and analyzed in section VI.

## II. MONITORING GETS

Two approaches have emerged attempting to solve the problem of monitoring GETs. The first, is the camera-based monitoring system where the GETs are continuously monitored by a special camera and with the help of real-time image processing algorithms, the system can extract information about the attachment state, wear level, and several other variables of the target GET. The second type is the WSN approach which depends on wireless sensing nodes integrated within the GET's structure to directly collect and transmit sensory data.

Camera solutions [7] [8] are prone to measurement errors because of the inherent uncertainty in the visual scene. While machine learning algorithms can improve their accuracy, such algorithms are only as good as their training data sets. Also, the variability of images among different weather, illumination, and operating conditions can considerably limit the reliability of camera-based systems. Furthermore, the required computing power for camera solutions becomes fairly significant as the system scales up.

WSN solutions have been proposed to actively monitor the GET by direct measurements [9]. Furthermore, early basic implementations are starting to surface [10].

Integrating Wireless Sensors (WSs) inside the GETs is an appealing solution and it has the potential to bring several secondary benefits along with its primary purpose of monitoring the mechanical integrity of GETs. An integrated WS can cheaply sense several physical quantities and use them as indicators for a number of other important operational variables. For example, a vibration sensor can indicate equipment utilization, a simple probe or an ultrasonic sensor can measure the wear level [11], and an Inertial Measurement Unit (IMU) can monitor the operational cycle to track the productivity of the whole equipment. Also, sensor integrated GETs are not affected by weather conditions or site illumination.

### III. CASE STUDY

#### A. Oil Production Process

Mining oil-sands in Canada, is a complex process that requires numerous critical factors to be in tune for the process to stay economically viable. It starts with massive electric-rope shovels (payload  $\approx 100$  metric ton) digging the ore out of the ground as shown in Fig. 1. Then a large fleet of hauler trucks carries the ore back to the processing plant. The rock crusher represents the very first stage in the plant. Its function is to grind the mined rocks down to manageable sizes. The crusher is operational around the clock and its down time is a direct cause for production cuts.

One of the major reasons for the crusher's down time is the unnoticed presence of scrap steel chunks in the ore. These chunks of steel jams the crusher and causes serious damage. Often during the dig, a shovel adapter/tooth will break, fall in the hauler truck, and end up in the inlet of the crusher, resulting in a significant maintenance bill and a few hours of halted production.

#### B. Monitoring System

The solution demanded for a reliable way of detecting detached adapters/teeth and reporting such events in real-time before they end up in the crusher. As shown in Fig. 1, the system consists of two types of wireless nodes: SeNs and SiNs. The SeNs are installed on the shovel's adapters and equipped with a special radio (LoRa™) while SiNs are installed in the cabin and on light poles along the way to the crusher. The SiN has two wireless interfaces; LoRa™ and 4G-LTE. The 4G-LTE link enables all the SiNs to communicate with the back end server while LoRa™ enables long-range communication with the SeNs.

Unfortunately, the structure of the tooth did not have any exploitable cavities for housing a SeN. Thus, our SeN only detects adapter detachments which are far less common. During normal operation, the SeNs are continuously reporting to the SiN installed on the shovel's cabin. In case of a detachment, the SeN will detect it and report it back to the SiN which will alarm the shovel operator in the cabin. If the SeN was damaged in the event, then the SiN will produce the

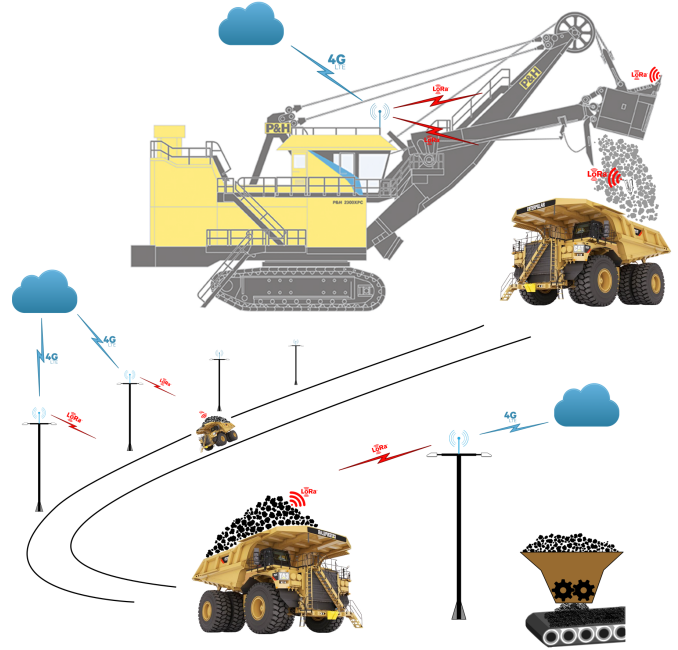


Fig. 1. Process Overview. Wireless links highlighted in red are LoRa™, while those highlighted in pale blue are 4G-LTE data connections. The crusher is at the lower right corner. The blue cloud represents the back-end cloud server.

alarm after a preset period (seconds) of detected radio silence from the damaged node. Along the way from the shovel to the crusher, several SiNs are installed on light poles to detect and track the signal of any detached adapter in the payload of any passing truck. If one of these SiNs picked up a signal, the cellular network is used to send an alarm to the crusher's control room. This will allow operators to track and divert the suspected truck away before it dumps its payload in the crusher.

### IV. SENSOR NODE

The SeN is composed of 5 components: sensing, control, communication, power supply, and the protective package. The design and development took numerous iterations (5 Printed Circuit Board (PCB) revisions and 3 package designs) to develop the required functions and achieve all the performance goals. This application required the node's hardware to tolerate several harsh operating conditions: First, extreme temperatures ( $-40 \rightarrow 80^\circ\text{C}$ ) dictated by the very cold Canadian winter on one side, and the significant heat created by the friction forces during digging on the other side. Second, excessive vibrations which are projected to be on the very low frequency end ( $<100$  Hz). Third, dirty and wet conditions typically present in a digging site.

#### A. Control

The control unit is merely an ultra low power microcontroller (Texas Instruments: MSP432P401R). It is interfaced with all the sensors, and the LoRa™ transceiver. It spends most of its time in a deep sleep mode to save energy (current



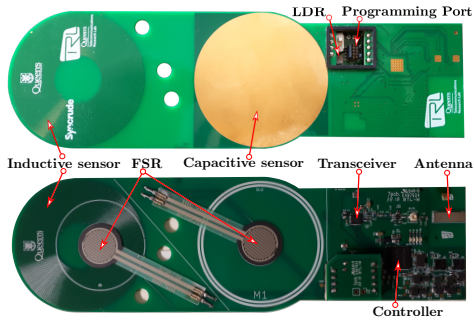


Fig. 2. PCB of the SeN. Stacking four 1-oz copper layers, impedance matching for RF traces, 1.6mm thick FR-4 fibreglass.

consumption down to 150 nA). It wakes up only when two conditions are met: First, the shovel is actively digging. Second, it is due for sending a new data packet to the SiN.

The controller's firmware handles low level sensing functions as well as the Medium Access Control (MAC) protocol managing the LoRa™ transceiver. The system utilizes a custom made MAC protocol which was the subject of separate works [12] [13].

### B. Sensing

The sensing unit is composed of 5 types of sensors. Most of them are used to detect the proximity of the adapter to the shovel's bucket. The multiplicity of proximity sensors provided enough redundancy to reliably measure the most important monitored variable. Also, the types of proximity sensors were diverse in their sensing mechanism. This allowed for field testing several types and configurations of sensors at the same time.

#### 1) Proximity sensors.

These sensors probe the proximity of the shovel's bucket to the internal cavity of the adapter.

- Capacitive [14].

The self-capacitance ( $C_s$ ) of a big circular copper pad changes in response to the proximity of any conductive surface. The pad is connected to a resonant circuit and a capacitance to digital converter (CDC) (Texas Instruments: FDC2214) measures the resonant frequency and use it to calculate  $C_s$ .

- Inductive.

Similarly, the inductance ( $L$ ) of a 4-layers PCB coil changes in response to the proximity of any conductive surface. The PCB coil is again connected to a resonant circuit where an inductance to digital converter (IDC) (Texas Instruments: LDC1614) is used to measure the resonant frequency and then calculate  $L$ .

- Magnetic force.

This is a custom made sensor designed to measure the proximity of a ferrous target by measuring the magnetic force exerted on a strong neodymium magnet embedded in the sensing node. The force is measured using a force sensing resistor (FSR)

however, the capacitance of the FSR was utilized instead of its resistance. This sensor is the subject of a separate work [15].

#### 2) light sensor.

A Light Detecting Resistor (LDR) is used to sense the intensity of incident light on the SeN. When the adapter is intact and fully attached to the bucket, the light entering its internal cavity (where the SeN is installed) is expected to be minimal. On the contrary, when the adapter is broken/detached, the SeN will be exposed to more light. The difference in ambient light between day and night necessitates time stamping of all measurements in order to use the right thresholds.

#### 3) Vibration sensor.

An omnidirectional vibration sensor (Sensolute: MVS0409.02) allows for detecting the operational state (idle vs active) of the shovel. This enables the controller to enter a deep sleep mode whenever the shovel is idle to save energy. This sensor is necessary because the controller can only wake up from a deep sleep mode by an external interrupt signal.

#### 4) Temperature sensor.

The operating temperature of the SeNs is  $-40^\circ$  to  $85^\circ\text{C}$ . To support troubleshooting in case of a node failure, the operating temperature is regularly reported.

#### 5) Battery voltage sensor.

The battery has sufficient capacity to power the SeN throughout its estimated life-time ( $\approx 1$  year) however, in subzero temperatures, the battery can lose a lot of its capacity ( $\approx 50\%$  at  $-40^\circ\text{C}$ ). A voltage sensor integrated in the microcontroller allows the system to keep an eye on the battery and evaluate its performance under various operating temperatures.

### C. Communication

Establishing a reliable wireless link between the sensor and the SiN was a challenge because the SeN's antenna is enclosed in a steel cavity which acts as a Faraday cage trapping electromagnetic radiation. Modifying the structure to allow for efficient radiation was forbidden. Luckily, mechanical clearances allowed for a non-hermetic cavity with gaps (a few millimetres thick) along the edge of the adapter's arm. These gaps were exploited to get the signal to escape the cavity with enough power to reach its destination (25 meters away) reliably. LoRa™ was chosen specifically because it provided superior link budget at the cost of low data rates. The extreme signal attenuation introduced by the adapter required a significant wireless link budget. Also, the data payload was very small and could be easily handled by a low rate connection. The subject of wireless communication from within a non-hermetic metallic enclosure is discussed in a separate work [16].

### D. Power Supply

The constraints of this system required a battery with a special set of features: Small size, high capacity, very low

operating temperature (down to  $-40^{\circ}\text{C}$ ). Also, a minimum of one year lifetime was required for the SeN. It was the tightness of the energy budget that sparked the work of a custom MAC protocol [12] [13]. This protocol along with the careful choice of battery, allowed for achieving the required lifetime. The battery contained three cells, each with a rated capacity of 2.6 Ah (SAFT: LS14500). Thus, the total capacity is 7.8 Ah.

### E. Protective Package

The protective package shown in Fig. 4 protected the PCB and the battery from harsh operating conditions (Water, dust, vibration, and mechanical shocks). It is composed of four components.

- 1) **Silicone rubber:** Used for potting the PCB to dampen vibrations and mechanical shocks. In a lab test, the SeN successfully tolerated a 8.8 metric ton impact force without any loss in functionality or performance. However, The rubber shifted the input impedance of the antenna and caused a considerable impedance mismatch. Therefore, the onboard matching network was tuned to compensate for the difference in relative permittivity  $\epsilon_r$  between air and silicone rubber. The type used (MoldMax: 14NV) was chosen for its low  $\epsilon_r$  (3.4 at 100 Hz), low dissipation factor (0.02 at 100 Hz), wide range of operating temperature ( $-53 \rightarrow 204^{\circ}\text{C}$ ), and no requirement for vacuum degassing. The system was strictly constrained from modifying the structure of the adapter in any way. Therefore, the package had to be an exact fit to the internal cavity of the adapter. To achieve this, we started by laser scanning the adapter to produce a 3D CAD model as shown in 3. Then, we used the CAD model to create a tightly fitting mold for potting the rubber. The mold was then 3D printed and post processed to smooth its surface.
- 2) **The FR-10 plate:** It is a thick (3 mm) high-strength fibreglass plate (FR-10). It protects the package from high mechanical loads by transferring them to the perimeter of the adapter's cavity while having a minimal effect on the antenna.
- 3) **The Polycarbonate support:** Used for supporting the FR-10 plate from the back side. It was 3D printed from a polycarbonate filament to have high compression strength. Then, it was glued to the FR-10 plate using a structural acrylic adhesive (PermaBond: TA4246).
- 4) **The fibreglass sleeve:** This is a thin (0.2 mm) resin-coated fibreglass sleeve used to hold the rubber and the FR-10 plate together as well as provide an extra layer of protection.

The programming window was used to for debugging the firmware up till the deployment. At this point the window was sealed with optically clear epoxy to enable ambient light to reach the LDR inside.

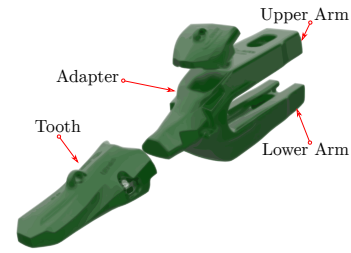


Fig. 3. The adapter/tooth assembly of the designated electric-rope shovel.

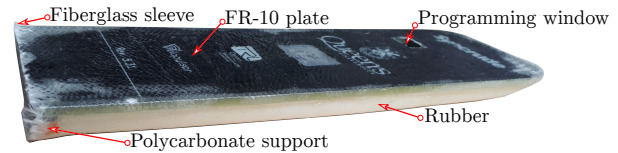


Fig. 4. The SeN potted in silicone rubber, covered with and FR-10 (3 mm) fibreglass plate and wrapped with a thin (0.2 mm) resin coated fibreglass sleeve.

## V. SINK NODE

The SiN houses several hardware modules as shown in Fig. 5. The Raspberry Pi 4 (RPI) is a Single Board Computer (SBC) running Linux and serves as the central manager of all the other modules. It connects over Wi-Fi to the cabin mounted tablet shown in Fig.10. A Hardware Attached on Top (HAT) is a standard hardware module that can be stacked on top of the RPi. In this setup, the RPi has three HATs: First, the 4G-LTE HAT (Quectel EC25-A) which houses a data enabled sim-card (Twilio) and allows for a connection through cellular networks to the back-end server. Second, the uninterruptible power supply (PiJuice) supported by a lithium-ion battery (5 Ah) to make sure the SiN will remain online (for a few hours) in case the power cable got disconnected. This allows for backing up any queued data and safely shutting down the SiN until power is restored. Third, the LoRa™ gateway (RHF0M301) which connects to all the SeNs in a star topology over multiple channels in the Industrial, Scientific & Medical (ISM) band of  $902 \rightarrow 928$  MHz. All the hardware was housed in a weather proof (IP67) box.

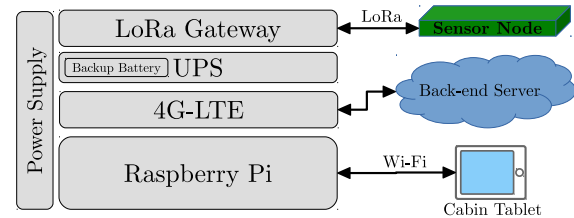


Fig. 5. Block diagram of the SiN hardware setup.

## VI. FIELD TEST

The field test had to be planned carefully and executed quickly to avoid any unnecessary downtime for the shovel and minimize costly production cuts. The test started at the workshop where a couple of SeNs were installed on an adapter. In

order to simplify and speed up installation, strong neodymium magnets (K&J Magnetics: MM-A-48) were placed inside the sensor's package. These magnets allowed for installing the SeN inside the adapter's cavity by just latching it.

Then the adapter was repeatedly attached/detached to/from an idle bucket while readings were collected and compared to the timed events log created by the observing team. Each round took about 6 minutes to complete. Fig. 6 shows an example of the data collected from one round of the workshop test. The readings are expressed as raw outputs from the analog to digital converter. It is worth mentioning that in a few cases, the adapter would be partially detached while some or all the sensors are indicating otherwise. This is because in these few cases, the proximity sensors were still able to detect the bucket's presence even when the adapter was not fully inserted. This means that individual sensors may not detect partial detachments but will reliably detect a complete detachment which was the case every time.

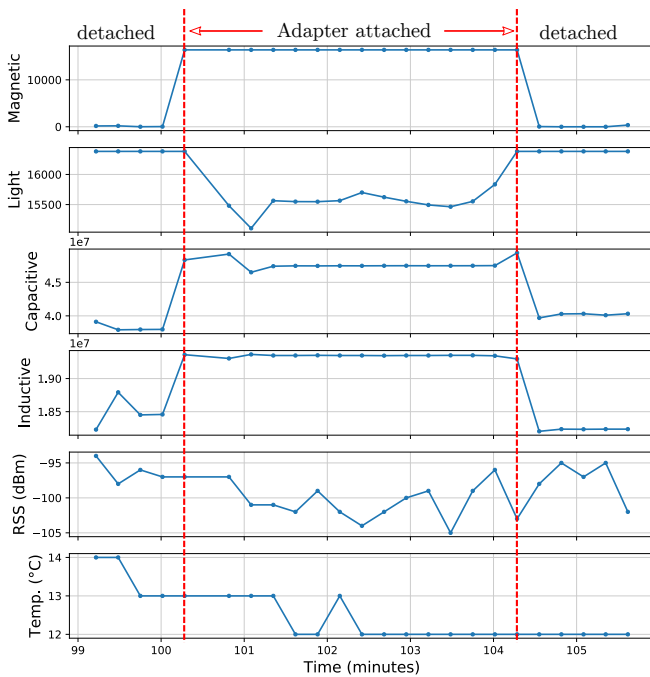


Fig. 6. Sensor readings from an attaching/detaching test in the workshop.

After the workshop test was concluded. The system was deemed ready for a test on an operational shovel. Consequently, a low priority shovel was assigned which was later stopped and sensor-equipped adapters were installed on its bucket as shown in Fig. 7. This shovel test ran for a much longer duration (3 hr).

After installing the SeNs, The SiN was mounted on a rail right next to the operator's cabin. A Yagi array which boosted the wireless link budget by 14 dB was used with the LoRa™ transceiver of the SiN. The location of the SiN relative to the bucket is shown in Fig. 8. The range is about 25 m and with a highly sensitive receiver (down to  $-140$  dBm) the wireless link budget was enough for a reliable connection.



Fig. 7. The SeN inside the adapter while it is lifted and being attached to the bucket on an operational shovel.



Fig. 8. A photo from the SiN's location on a rail next to the cabin. The LoRa™ transceiver used a Yagi array for its high gain and directivity which added an extra 14 dB to the wireless link budget.

The sensors were up and running before being installed on the adapters. Initially, the sensors were inside the cabin of a pickup truck with its heat turned on. In Fig. 9, this is demonstrated by the room temperature readings during the first few minutes ( $\approx 23$  °C) followed by a downward trend towards the ambient air temperature on that day ( $\approx 8$  °C). It took more than 20 minutes for the core temperature of the SeN to reach that of the ambient air. This is due to the low thermal conductivity of the packaging rubber (0.21 W/mK). After digging started (around minute 67), the friction caused the adapters to heat up. We can notice the slowly increasing temperature as the heat propagates to the inner core of the SeN.

The light sensor performed as expected in the workshop test as shown in Fig. 6. A similar behaviour was noticed later when the adapter got attached to the bucket and before the shovel started digging. On the contrary, when the digging started, the readings fluctuated significantly as shown in Fig. 9.

The magnetic sensor showed a steady response in the workshop and on the digging shovel. While this sensor is the most expensive among all the proximity sensors, it has the most reliable output. The distinction between both states (attached/detached) of the adapter is very clear. The reason for this clear distinction is that the neodymium magnet inside this sensor was chosen so that the anticipated proximity range of the bucket would cause it to saturate the FSR. This is explained in more details in [15].

Capacitive and inductive sensors exhibit a similar behaviour. Once again, their output before the shovel started digging is very close to their output in the workshop. After digging started, we notice marginal fluctuations in their readings however, there is still a clear distinction between the two states (attached/detached). These fluctuations are attributed to the wiggling motion of the adapter with respect to the bucket.



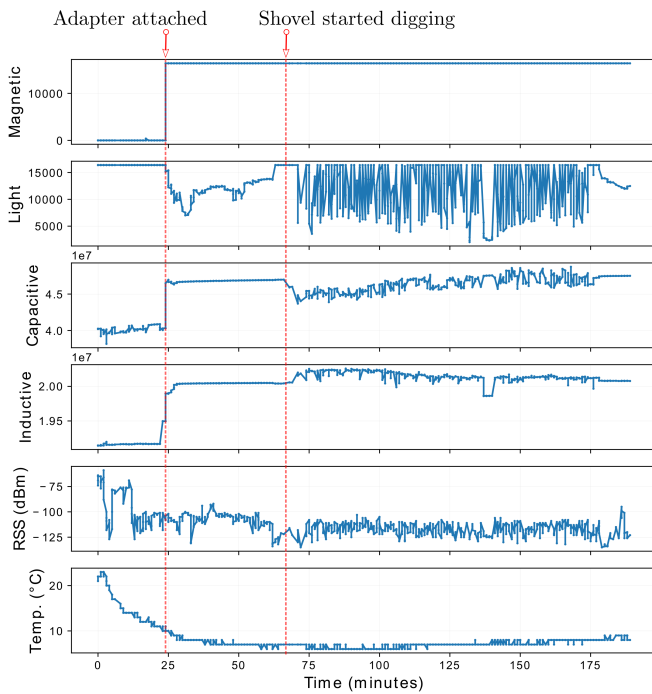


Fig. 9. Sensor data collected from an operational shovel during the field test.

Since both of these sensors have a sub-millimetre resolution, they were able to pick up the wiggling motion.

During the numerous attachment/detachment tests in the workshop, the detection rate was 100% for all the proximity sensors except the light sensor whose rate was 80%. As for the active shovel test, the light sensor failed to detect attachment while the capacitive and inductive succeeded with a reasonable margin and the magnetic with an excellent margin.

Status of individual adapters are displayed on the cabin tablet as shown in Fig. 10. It is constantly receiving sensory data in real-time from the SiN through a Wi-Fi connection. The tablet was added to the system to provide a convenient graphical interface for the operator. It produces audible and visual alarms whenever a detachment is detected and specifies the location of the missing adapter.

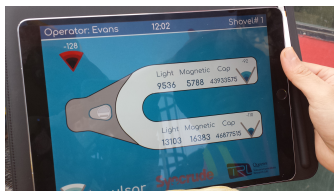


Fig. 10. Operator dashboard on the cabin tablet. Sensor readings from both nodes are shown on their respective adapter's arm along with their Received Signal Strength (RSS) in dBm on the right.

Going through a full development cycle up to field testing revealed several system limitations that would not have been exposed otherwise. For example, the SeNs required careful assembly and packaging which consumed significant manual labour time. This raises concerns of mass manufacturing the

SeNs on a wide scale. Also, SeNs' disposal at the end of their service life may have a negative environmental impact because of the integrated batteries.

## VII. CONCLUSION

A complete system to monitor GETs was demonstrated. A WSN was designed and implemented to monitor the GETs of an electric-rope shovel. Field testing results showed a reliable wireless link and a rugged hardware platform. The SeN successfully detected and reported all emulated detachments. The rugged package successfully tolerated harsh conditions during active operations in an oil-sand mine. Allowing structural adjustments to the GET for hosting WSs will boost the link budget and consequently enhance the energy efficiency of the SeNs and extend their life-time. The presented design techniques paves the way for developing wireless sensing hardware platforms for harsh environments.

## REFERENCES

- [1] K. Zhou, T. Liu, and L. Zhou, "Industry 4.0: Towards future industrial opportunities and challenges," in *2015 12th International Conference on Fuzzy Systems and Knowledge Discovery (FSKD)*, Aug. 2015, pp. 2147–2152.
- [2] Y. Lu, "Industry 4.0: A survey on technologies, applications and open research issues," *Journal of Industrial Information Integration*, vol. 6, pp. 1–10, Jun. 2017.
- [3] N. Srivastava, "Challenges of Next-Generation Wireless Sensor Networks and its impact on Society," vol. 1, no. 1, p. 6, 2010.
- [4] G. Saha, "Abrasive wear of alloys for ground engaging tools," Ph.D. dissertation, Deakin University, Sep. 2017. [Online]. Available: <http://dro.deakin.edu.au/view/DU:30103712>
- [5] C. Subramanian, "Fatigue Failure of a Ground-Engaging Tool," *Journal of Failure Analysis and Prevention*, vol. 9, no. 2, pp. 122–126, Apr. 2009.
- [6] P. Burke, "When the best laid plans go awry," *MineSafe Magazine*, vol. 16, no. 3, pp. 33–34, Dec. 2007.
- [7] E. L. Bewley, N. Cowgill, and J. E. Blomberg, "Wear part monitoring," U.S. Patent 9670649, Jun., 2017. [Online]. Available: <https://patents.google.com/patent/US9670649B2/en>
- [8] "Motion Metrics." [Online]. Available: <https://www.motionmetrics.com/>
- [9] A. El Kouche, A. Alma'aitah, H. Hassanein, and K. Obaia, "Monitoring operational mining equipment using Sprouts Wireless Sensor Network platform," in *2013 9th International Wireless Communications and Mobile Computing Conference (IWCMC)*. Sardinia, Italy: IEEE, Jul. 2013, pp. 1388–1393.
- [10] "G.E.T. Detect." [Online]. Available: <http://www.esocorp.com/EN/escoiq/Pages/GETDetect.aspx>
- [11] A. E. Kouche, "Towards a wireless sensor network platform for the Internet of Things: Sprouts WSN platform," in *2012 IEEE International Conference on Communications (ICC)*, Jun. 2012, pp. 632–636.
- [12] G. Hassan and H. S. Hassanein, "MoT: A Deterministic Latency MAC Protocol for Mission-Critical IoT Applications," in *2018 14th International Wireless Communications Mobile Computing Conference (IWCMC)*, Jun. 2018, pp. 588–593.
- [13] G. Hassan, M. ElMaradny, M. A. Ibrahim, A. M. Rashwan, and H. S. Hassanein, "Energy Efficiency Analysis of Centralized-Synchronous LoRa-based MAC Protocols," in *2018 14th International Wireless Communications Mobile Computing Conference (IWCMC)*, Jun. 2018, pp. 999–1004.
- [14] L. K. Baxter, *Capacitive Sensors: Design and Applications*, ser. IEEE Press Series on Electronics Technology. IEEE, 1997.
- [15] M. A. Ibrahim, G. Hassan, K. Monea, H. S. Hassanein, and K. Obaia, "A Ferrous-Selective Proximity Sensor for Industrial Internet of Things," in *IEEE International Conference on Communications (ICC)*, Jun. 2020.
- [16] M. A. Ibrahim, G. Hassan, H. S. Hassanein, and K. Obaia, "A wireless sensor platform for industrial non-hermetic metallic enclosures," in *2017 13th International Wireless Communications and Mobile Computing Conference (IWCMC)*, Jun. 2017, pp. 165–170.